ELSEVIER

Biochimica et Biophysica Acta 1229 (1995) 225–232

BBA Biochimica et Biophysica Acta

F_1-ATPase α-subunit made up from two fragments (1–395, 396–503) is stabilized by ATP and complexes containing it obey altered kinetics

Masahiko Miyauchi, Kaeko Tozawa, Masasuke Yoshida *

Research Laboratory of Resources Utilization, Tokyo Institute of Technology, Nagatsuta 4259, Yokohama 227, Japan

Received 19 October 1994; accepted 19 December 1994

Abstract

Inferred from the crystal structure of mitochondrial F_1-ATPase (Abrahams, J.P. et al. (1994) Nature 370, 621–628), the proteinase-sensitive region around Phe-395 of thermophilic F_1-ATPase α-subunit corresponds to the loop which connects main part of the carboxyl-terminal helical bundle domain with the ATP binding domain. This loop is in contact with the γ- and adjacent β-subunits. Two polypeptides corresponding to the sequence 1–395 and 396–503 of the α-subunit were expressed in *Escherichia coli* cells and they were copurified as an apparently functional α-subunit (α(395/396)) made up of two polypeptides. The isolated α(395/396) was stabilized by ATP-Mg, but not by ADP-Mg, although it bound both ATP-Mg and ADP-Mg with similar affinities (K_d, 11 μM and 14 μM, respectively). The α(395/396) was reconstitutable into α(395/396)$_3\beta_3$ and α(395/396)$_3\beta_3\gamma$ complexes. Different from the intact $\alpha_3\beta_3$ complex, the α(395/396)$_3\beta_3$ complex was significantly resistant to the ATP-Mg-induced dissociation into $\alpha_1\beta_1$ heterodimers. ATP hydrolysis by the α(395/396)$_3\beta_3\gamma$ complex underwent a slow initial phase, whereas the intact $\alpha_3\beta_3\gamma$ complex exhibited an accelerated initial phase. Steady-state ATPase activity at various ATP concentrations showed negative cooperativity for the intact $\alpha_3\beta_3\gamma$ complex but apparently positive cooperativity for the α(395/396)$_3\beta_3\gamma$ complex. The ATPase activities at a saturating ATP concentration of the complexes containing the α(395/396) were 180% of those containing intact α-subunits. These results indicate that a loop around Phe-395 is involved in intersubunit interaction in F_1-ATPase.

Keywords: ATPase, F_1-; ATP binding domain; Alpha subunit; Subunit interaction

1. Introduction

The H^+-ATP synthase is responsible for ATP synthesis at mitochondria, chloroplasts and bacterial plasma membranes. It is composed of two portions, an integral membrane portion, F_o, and a peripheral portion, F_1 [1–4]. F_o is a proton channel and F_1 is a soluble catalytic portion (F_1-ATPase) which is composed of five kinds of subunit called α (55–57 kDa), β (50–54 kDa), γ (30–38 kDa), δ (15–19 kDa) and ϵ (6–15 kDa) with a stoichiometry of $\alpha_3\beta_3\gamma_1\delta_1\epsilon_1$. Isolated α- and β-subunits can bind AT(D)P, but neither of them can hydrolyze ATP. These two subunits have almost the same folding topology [5,6] and are arranged in a hexagonal array with juxtaposition in F_1-ATPase. The minimum unit of the subunit complex that has ATP hydrolyzing activity is $\alpha_3\beta_3$ or $\alpha_1\beta_1$ complexes [7–9]. The catalytic sites are present mostly on the β-subunit and hence the AT(D)P binding site detected for the isolated β-subunit becomes the catalytic site when β-subunits are assembled into holo-enzyme [10]. Our understanding of the role of α-subunits is more obscure than that of the β-subunit, even though its regulatory function through α–β-subunit interaction has been suggested. Analysis of mutations of F_1-ATPase α-subunit from *Escherichia coli* and other organisms showed that at least three regions in the α-subunit are involved in regulation of ATPase activity. These are: a nucleotide binding consensus sequence region around Lys-175 [1] [11–14], the region

Abbreviations: TF_1, F_1-ATPase from thermophilic *Bacillus* strain PS3; C2-loop, water accessible region from Glu-393 to Phe-398 of TF_1-α-subunit; C2-subdomain, a carboxyl-terminal subdomain comprising about 105 residues; $\alpha(\sim 395)$, an amino-terminal 42 kDa peptide fragment which consists of amino acids from amino-terminal to Phe-395 of TF_1-α-subunit; $\alpha(396\sim)$, a carboxyl-terminal 12 kDa peptide fragment which consists of amino acids from Ala-396 to carboxyl-terminal of TF_1-α-subunit; α(395/396), TF-α-subunit whose peptide bond between Phe-395 and Ala-396 is cleaved; SDS, sodium dodecyl sulfate; PAGE, polyacrylamide gel electrophoresis; HPLC, high-performance liquid chromatography.

* Corresponding author. Fax: +81 45 9245277.

[1] Numbering of residues of F_1-ATPase α-subunits in this paper is according to that of TF_1-α-subunit.

SSDI 0005-2728(95)00004-6

around Pro-281–Ala-285 [15], and the region around Arg-365–Arg-376 [16–20]. Mutations occurred to these regions produced F_1-ATPase which showed altered kinetic cooperativity, partial or nearly complete loss of ATPase activity, or decreased stability.

We reported previously an extensive analysis of limited proteolysis of the isolated α-subunit of F_1-ATPase from a thermophilic *Bacillus* strain PS3 $(TF_1)^2$ and proposed the location of eleven water-exposed loop regions [6]. Among them, three loops are extremely sensitive to proteolysis. They are the regions around Glu-20, Arg-283 and Phe-395. The α-subunit retains its gross structure even after cleavage of the peptide chain at these regions. The region around Glu-20 is a loop connecting a short amino-terminal region to the main part of the α-subunit and this short peptide region, of which corresponding sequence is absent in the β-subunit, is essential for the binding of the α-subunit to the δ-subunit [21,22]. The second region around Arg-283 is overlapped with the region probed by mutagenesis as described above. The third region around Phe-395, designated as the C2-loop [6], connects a carboxyl-terminal subdomain comprising ~ 105 residues (C2-subdomain) to the rest part of the α-subunit. Recent achievement of X-ray crystallography of mitochondrial F_1-ATPase clearly shows that the regions around Arg-283 and Phe-395 are indeed loops which can interact with the γ-subunit and adjacent β-subunits (Fig. 1) [5]. The ATPase activity of the $\alpha_3\beta_3$ complex reconstituted from the proteinase-treated α-subunit, of which major population had a peptide chain cleavage at the C2-loop, was 140–250% of that of intact $\alpha_3\beta_3$ complex. These results suggest that the C2-loop of α-subunit is likely to be involved in the regulation of ATPase activity in F_1-ATPase [6]. However, one of the drawback of the previous work is that we used proteinase-treated α-subunit which was inevitably a mixture of proteins with different degree of proteolysis. Here, we have expressed two peptide fragments corresponding to the sequence 1–395 ($\alpha(\sim 395)$) and 396–503 ($\alpha(396 \sim)$) of the TF_1-α-subunit in *E. coli*. Two peptides associated each other spontaneously in *E. coli* cells and were copurified as an apparently functional α-subunit ($\alpha(395/396)$). Using this homogeneous preparation, we studied effect of introduction of a peptide chain nick at the position between 395 and 396 of the α-subunit (Fig. 1, an arrow) on the stability and kinetics of the reconstituted $\alpha_3\beta_3$ and $\alpha_3\beta_3\gamma$ complexes.

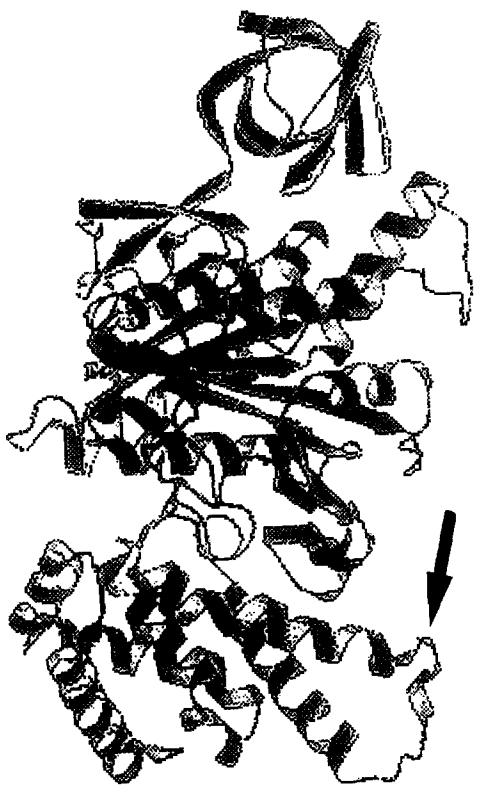

Fig. 1. One of α subunits ('α_{TP}' in Ref. 5) is depicted from the structure of mitochondrial F_1-ATPase. The site corresponding to the peptide chain nick between Phe-395 and Ala-396 in TF_1-α subunit studied in this paper is indicated by an arrow. The C2-loop is a loop containing the indicated peptide chain nick and the C2-subdomain is a region containing Ala-396 to the carboxyl-terminus, a bundle of α-helices.

2. Experimental procedures

2.1. Expression and Isolation of $\alpha(395/396)$

The plasmid to express two peptides, $\alpha(\sim 395)$ and $\alpha(396 \sim)$, was constructed from pTDT7α [23] by oligonucleotide-directed mutagenesis [24]. A 38 mer oligonucleotide used for mutagenesis was (5′)GAATTG-GGCCATATGGGTACCTCCTTAGAACGCTTCGA(3′). The underlining indicates the newly inserted sequence. It was designed to have a stop codon (TTA, complementary sequence), a ribosome-binding (Shine-Dalgarno) sequence (ACCTCCT) and an initiation codon (CAT). This sequence was inserted between Phe-395 (GAA) and Ala-396 (GGC) of the TF_1-α-gene in the plasmid so that it can express two peptides simultaneously. For easy detection of mutants by agarose electrophoresis, the oligonucleotide also had a new restriction site, the *Nde*I site (CATATG). The mutant plasmid was transformed into *E. coli* BL21(DE3) (*hsd*S, *gal* (*lcI*857, *ind*1, *Sam*7, *nin*5, *lac*UV5-T7*gene1*)) strain and the transformed cells were cultured in 3 liters of 2 × YT medium at 37° C. Isopropyl 1-thio-β-D-galactoside was added to induce production of protein when absorbance at 595 nm of the culture reached 1.0 and culture was continued for another 15 h. Then, the cells were harvested by centrifugation and were suspended in 200 ml of 20 mM Tris-sulfate buffer (pH 8.0), containing 1 mM $MgCl_2$ and 3 mg of DNase. The cells were disrupted with sonication (5 min, 3 times) on ice. The suspension was centrifuged at 16000 rpm for 10 min and the supernatant was further centrifuged at 36000 rpm for 40 min. The two peptides recovered in the supernatant were purified by procedures used for the purification of the

intact α-subunit [13,25] except that DEAE-Toyopearl (superfine) column chromatography was added at the last step of the purification. Briefly, the supernatant was applied to a DEAE-Sephacel column. The protein was eluted with a linear gradient of 0–300 mM NaCl in 20 mM Tris-sulfate (pH 8.0) containing 1 mM EDTA. The second column was Toyopearl HW-55(F). The elution was performed with a linear decreasing gradient of 30–0% ammonium sulfate in 20 mM Tris-sulfate buffer (pH 8.0), containing 1 mM EDTA. The last step was DEAE-Toyopearl superfine column chromatography developed with a linear gradient of 0–200 mM NaCl in 20 mM Tris-sulfate buffer (pH 8.0), containing 1 mM EDTA. In the course of the purification, presence of the two peptides in the fractions was detected by the polyacrylamide gel electrophoresis in the presence of sodium dodecyl sulfate (SDS-PAGE).

2.2. Analysis of proteins

Proteins were analyzed on polyacrylamide gel electrophoresis in the absence (native-PAGE) or presence of 0.1% sodium dodecyl sulfate (SDS-PAGE) [26,27]. Concentration of polyacrylamide in native-PAGE was 7.5% and that in SDS-PAGE was 13%. Proteins in the gels were stained with Coomassie brilliant blue R-250. ATPase-activity staining of native-PAGE gel was carried out as described in [8,28]. In the case of two-dimensional electrophoresis, the first dimension was performed in native-PAGE and the second dimension was performed in SDS-PAGE. When the effect of ATP-Mg on the association of peptides was examined on native-PAGE, 1 mM ATP and 1 mM $MgCl_2$ were included in the gels and in the running buffer. Protein concentrations were measured with the dye-binding method of Bradford [29] using bovine serum albumin as a standard. The amino-terminal amino acid sequences were determined as described in [30].

2.3. Reconstitution of $\alpha_3\beta_3$ and $\alpha_3\beta_3\gamma$ complexes

The $\alpha_3\beta_3$ complex was reconstituted by incubation of α-(or α(395/396)) and β-subunits (each 10 mg/ml) in 20 mM piperazine-*N*,*N*′-bis(2-ethanesulfonic acid)-NaOH buffer (pH 7.0) containing 200 mM Na_2SO_4 at 30° C for 30 min. The $\alpha_3\beta_3\gamma$ complex was reconstituted as follows. The α- (or α(395/396)), β- and γ-subunits dissolved in the 20 mM piperazine-*N*,*N*′-bis(2-ethanesulfonic acid)-NaOH buffer (pH 7.0), containing 200 mM NaCl were mixed at final concentrations, 800, 800 and 100 μg/ml, respectively. Since solubility of γ-subunit is low, the mixture was slightly turbid. The mixture was incubated at 30° C overnight. The mixture containing reconstituted $\alpha_3\beta_3$ complex or $\alpha_3\beta_3\gamma$ complex was centrifuged at 40 000 rpm for 15 min and 100 μl of the supernatant was applied to gel-permeation HPLC. The peak fractions containing the complex were pooled and used for experiments on the same day as their preparation.

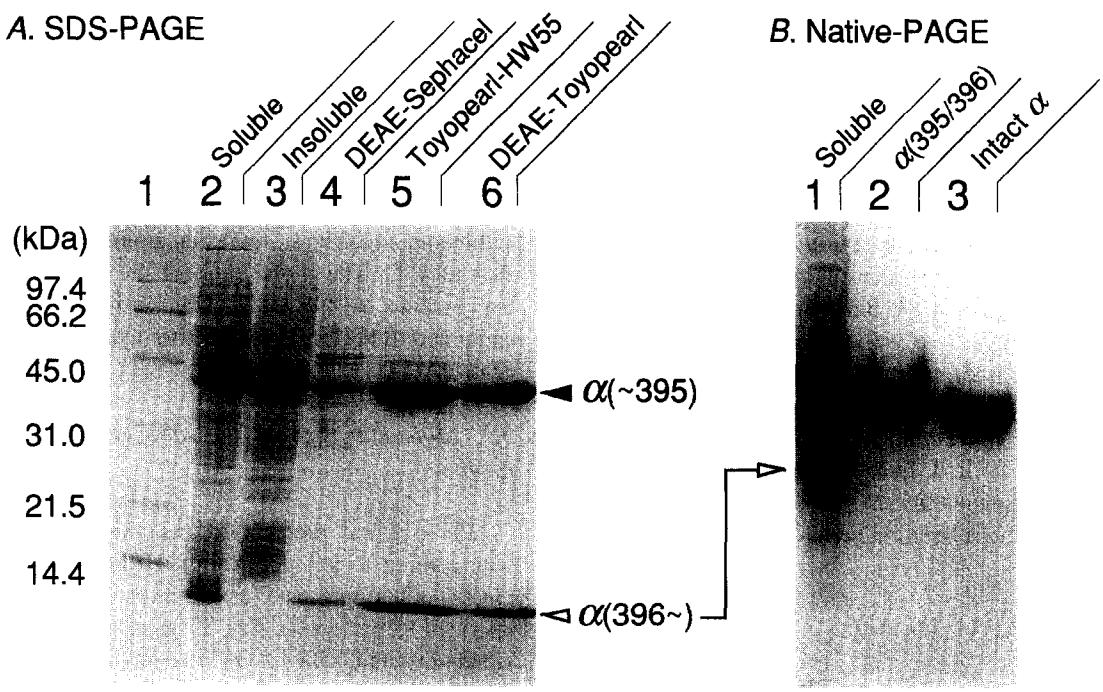

Fig. 2. Expression of the peptides α(~395) and α(396~) and purification of α(395/396). (A) SDS-PAGE analysis. Lane 1, molecular size markers (Bio-Rad). Lane 2, soluble fraction of expressed *E. coli*. Lane 3, insoluble fraction of expressed *E. coli*. Lane 4, enriched fraction after DEAE-Sephacel. Lane 5, enriched fraction after Toyopearl-HW55. Lane 6, purified α(395/396) fraction after DEAE-Toyopearl. (B) Native-PAGE analysis. Lane 1, soluble fraction of expressed *E. coli*. Lane 2, purified α(395/396) after DEAE-Sephacel. Lane 3, intact α-subunit.

2.4. Gel-permeation HPLC

The column (G3000SWXL, Tosoh, Tokyo) was equilibrated and eluted with 20 mM piperadine-*N,N'*-bis(2-ethanesulfonic acid)-NaOH buffer (pH 7.0) containing 200 mM Na_2SO_4 at a flow rate of 0.5 ml/min at room temperature. Free α- and β-subunit were eluted at 19.4 min and 18.7 min, respectively. For isolation of the $\alpha_3\beta_3\gamma$ complex, 200 mM NaCl was included instead of 200 mM Na_2SO_4. The reconstituted $\alpha_3\beta_3$ and $\alpha_3\beta_3\gamma$ complexes were eluted at 15 min. When indicated, 1 mM of AT(D)P-Mg were supplemented to the HPLC buffer.

2.5. Assay of ATPase activity

The ATPase activity was measured in the presence of ATP regenerating system. To compare ATPase activity of the reconstituted complexes containing intact α-subunit and $\alpha(395/396)$, we waited until the catalysis reached an apparent steady-state phase, usually at 600–800 s after initiating reaction, and measured the rate of ATP hydrolysis. The amount of enzyme was set between 5 and 10 μg per 1 ml of assay mixture. The assay mixture for $\alpha_3\beta_3\gamma$ complex contained 50 mM Tris-sulfate buffer (pH 8.0), 5 mM $MgCl_2$, 10 mM KCl, 3 mM phospho*enol*pyruvate, 20 μg/ml pyruvate kinase, 30 μg/ml lactate dehydrogenase, 150 μg/ml NADH, and 5 mM ATP unless otherwise indicated. In the case of the $\alpha_3\beta_3$ complex, 200 mM Na_2SO_4 was supplemented to stabilize the complex [7]. Reactions were initiated by the addition of the enzyme, and absorbance at 340 nm was monitored at 25° C. Values of ATPase activities were averages of several measurements. The activity which hydrolyzes 1 μmol of ATP per min is defined as 1 unit.

2.6. AT(D)P-induced UV difference spectra

UV difference spectra were measured at room temperature with a double-beam spectrophotometer UV-2200 (Shimadzu, Kyoto) using a pair of matched double cells with a light-pathlength of 4 mm for each compartment [31]. Intact α-subunit or $\alpha(395/396)$ was passed through a Sephadex G-50 (fine) column equilibrated with 10 mM Tricine-NaOH buffer (pH 8.0) containing 2 mM $MgCl_2$ before use. The concentrations of the α-subunit and $\alpha(395/396)$ were 10 μM. Every 2 μl of AT(D)P solution with appropriate concentrations was added to the protein solution according to a titration series.

3. Results

3.1. Expression of $\alpha(\sim 395)$ and $a(396 \sim)$ in E. coli

E. coli cells bearing the plasmid designed for expression of the peptides $\alpha(\sim 395)$ and $\alpha(396 \sim)$ produced two peptides with molecular sizes 42 kDa and 12 kDa in an isopropyl 1-thio-β-D-galactoside-inducible manner. When these protein bands in SDS-PAGE (Fig. 2A, lane 2) were subjected to the amino-terminal amino acid sequence analysis, the sequences S-I-R-A-E-E-I and A-Q-F-G-S-D-L were obtained for the 42- and 12-kDa peptides, respectively. These sequences agreed with those of the α-subunit from Ser-2 and from Ala-396, and thus the expression of the intended peptides was confirmed. Fortunately, initiator Met's were lost from both peptides and we did not have to consider the effect of additional Met ahead of Ala-396. The peptide $\alpha(396 \sim)$ expressed in *E. coli* was recovered only in the soluble fraction of disrupted cells. The peptide $\alpha(\sim 395)$ was found both in the soluble fraction and the insoluble fraction (Fig. 2A, lane 2, 3). Judged from staining intensity and the amount of proteins recovered in each of the fractions, about 90% of the peptide $\alpha(\sim 395)$ was recovered in the soluble fraction. When the soluble fraction was analyzed by native-PAGE in the presence of ATP, two distinct bands appeared (Fig. 2B, lane 1). The amino-terminal amino acid sequence analysis revealed that the upper band contained the two peptides and the lower band contained only the peptide $\alpha(396 \sim)$. Therefore, some proportion of the peptide $\alpha(396 \sim)$ in the soluble fraction existed as the unassociated, free form. The associated form of the two peptides in the supernatant was purified (Fig. 2A, lane 4–6). The purified peptides migrated as a single band in native-PAGE in the presence of ATP (Fig. 2B, lane 2). It seemed that some dissociation of the two peptides occurred during purification procedures and small amount of free $\alpha(\sim 395)$ and $\alpha(396 \sim)$ was found at each of the column chromatographies. For example, in the first DEAE-column chromatography, about 20% of the peptide $\alpha(396 \sim)$ and the peptide $\alpha(\sim 395)$ were eluted in non-adsorbed fractions and at 300 mM NaCl, respectively, while the remaining majority of the two peptides was eluted at 200 mM NaCl (data not shown). Once purified, the association of the two peptides was stable and could be stored as an ammonium sulfate suspension at 4° C. The molar ratio of the peptide $\alpha(\sim 395)$ to the peptide $\alpha(396 \sim)$ in the purified preparation was estimated to be 1:1.06 by densitometry of stained bands on SDS-PAGE.

3.2. Molecular size of the associated form of the two peptides

The purified preparation containing the two peptides was applied to gel permeation HPLC. The proteins were eluted as a single peak at the retention time which corresponded to molecular size 55 kDa, the same as the intact α-subunit, and SDS-PAGE analysis showed that this peak contained both peptides, $\alpha(396 \sim)$ and $\alpha(\sim 395)$ (data not shown). Therefore, we concluded that single copy of each of the two peptides associates into a 55 kDa protein. This protein can be thought of as a derivative of TF_1-α-

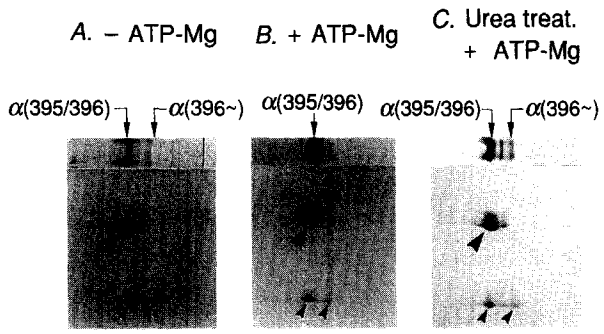

Fig. 3. Two-dimensional PAGE analysis of the effect of ATP-Mg on the stability of $\alpha(395/396)$ and association of the two peptides into $\alpha(395/396)$ after denaturation. Purified $\alpha(395/396)$ was applied to the first-dimension native-PAGE and successively to the second-dimension SDS-PAGE. Electrophoretic patterns of $\alpha(395/396)$ in the first dimension are shown at the uppermost of each electrophoregram. The positions of the peptides $\alpha(\sim 395)$ and $\alpha(396\sim)$ are indicated by large arrowheads and small arrowheads, respectively. (A) ATP-Mg was not included in the first dimension native-PAGE system. (B) 1 mM ATP-Mg was contained in the gel and in the running buffer of the first dimension native-PAGE. (C) Purified $\alpha(395/396)$ was dissolved in 8 M urea and incubated for 30 min at room temperature. The solution was applied directly to native-PAGE including 1 mM ATP-Mg. When proteins reached the lowest part of the stacking gel, electric current was stopped for 30 min, and then electrophoresis was resumed. Other experimental details are described in Experimental procedures.

subunit that has a peptide chain nick between Phe-395 and Ala-396 and we call the associated form of the two peptides as $\alpha(395/396)$ hereafter.

3.3. Stabilization of $\alpha(395/396)$ by ATP-Mg

When $\alpha(395/396)$ was analyzed by two-dimensional PAGE, some of the $\alpha(395/396)$ decayed into the two component peptides on the first dimension native-PAGE (Fig. 3A). However, when 1 mM ATP-Mg was included in the gel and in the running buffer of native-PAGE, almost all the peptides remained associated (Fig. 3B). This stabilizing effect was not observed for ADP-Mg (data not shown). These results indicate that $\alpha(395/396)$ is unstable and tends to decay during native-PAGE, and that ATP-Mg stabilizes the associated form and prevents it from decay. For this reason, native-PAGE for analysis of $\alpha(395/396)$ was carried out in the presence of ATP-Mg, unless otherwise stated.

3.4. Reassociation of the two peptides into $\alpha(395/396)$

When $\alpha(395/396)$ was dissolved in 8 M urea solution, the peptides were denatured and dissociated into each peptide. However, when this solution was directly applied to native-PAGE in the presence of 1 mM ATP-Mg, more than half of peptides were electrophoresed as $\alpha(395/396)$ (Fig. 3C). This indicates that the two peptides can fold and associate spontaneously with each other after complete denaturation in 8 M urea.

3.5. Binding of ADP-Mg to $\alpha(395/396)$

Binding of ADP-Mg to TF_1-α-subunit induces the characteristic difference UV spectra [31], and binding affinity of ADP-Mg to $\alpha(395/396)$ was estimated by this means. When 2–40 μM of ADP was mixed with 10 μM of α-subunit or $\alpha(395/396)$ in the presence of Mg^{2+}, difference spectra were induced with a peak at 276–278 nm and a trough at about 250 nm (Fig. 4). However, when the concentration of ADP-Mg was higher than 40 μM, 4-fold excess of concentration of the protein, the peak shifted to a shorter wave length and the shape of difference spectra became different from those below 40 μM of ADP-Mg (Fig. 4, dashed lines). When magnitude of difference spectra at the trough at 250 nm (ΔA_{250}) was subtracted from that of the peak at 278 nm (ΔA_{278}) and was plotted at ADP-Mg concentrations below 40 μM, the apparent K_d values 14 μM and 11 μM were obtained for $\alpha(395/396)$ and intact α-subunit, respectively. The K_d value of intact α-subunit was consistent with the previously reported one [31]. The same experiments were repeated for ATP-Mg and 11 μM and 8.8 μM were obtained as K_d of the $\alpha(395/396)$ and intact α-subunit, respectively. Thus, $\alpha(395/396)$ can bind ADP-Mg and ATP-Mg with similar affinities to those observed for the intact α-subunit.

3.6. Reconstitution of $\alpha(395/396)_3\beta_3$ and $\alpha(395/396)_3\beta_3\gamma$ complexes

When the mixture of $\alpha(395/396)$ and TF_1-β-subunit were incubated and applied to gel permeation HPLC, a protein complex with a molecular size 300 kDa, which contained approximately equal molar amounts of $\alpha(\sim 395)$, $\alpha(\sim 396)$ and the β-subunit, was eluted (Fig. 5a). This corresponds to a $\alpha(395/396)_3\beta_3$ complex, and thus, similar to the intact α-subunit [7], $\alpha(395/396)$ has the

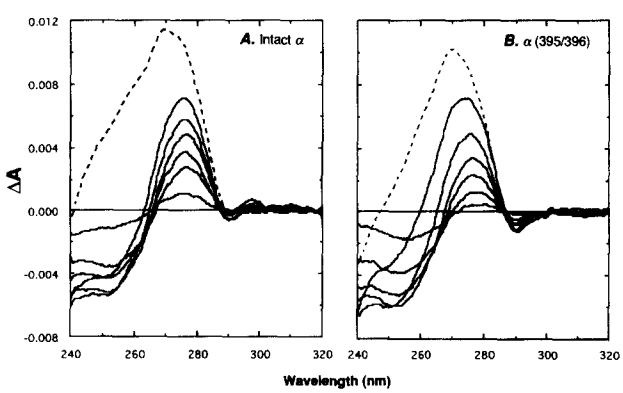

Fig. 4. ADP-induced difference UV spectra of intact α-subunit and $\alpha(395/396)$. A small aliquot of concentrated ADP solution was sequentially added to 10 μM of (A) intact α-subunit or (B) $\alpha(395/396)$ and spectral change was measured. Concentrations of ADP (from the lower spectra) were (A) 1.92, 5.73, 9.50, 13.3, 20.7, 35.3, 57.0 μM and (B) 1.99, 5.95, 9.87, 13.8, 21.5, 36.6, 44.2 μM. Other experimental details are described in Experimental procedures.

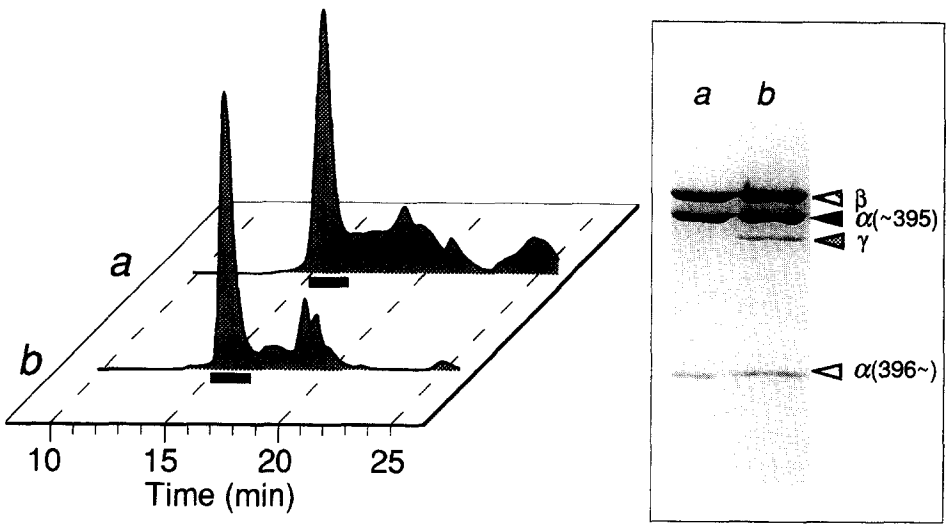

Fig. 5. Reconstitution of $\alpha(395/396)_3\beta_3$ and $\alpha(395/396)_3\beta_3\gamma$ complexes. The mixtures of (a) $\alpha(395/396)$ and β subunit and (b) $\alpha(395/396)$, β, and γ subunits treated as described in Experimental procedures were analyzed with gel permeation HPLC on a G3000SWXL column. Elution was monitored by absorbance at 280 nm and fractions indicated by bars were analyzed by SDS-PAGE.

ability to bind to the β-subunits to form an $\alpha_3\beta_3$ complex. As expected, when the mixture contained TF_1-γ-subunit in addition to $\alpha(395/396)$ and TF_1-β-subunit, the $\alpha(395/396)_3\beta_3\gamma$ complex was reconstituted (Fig. 5b). These results provide further evidence that the conformation of $\alpha(395/396)$ is similar to that of the intact α-subunit.

3.7. Stability of $\alpha(395/396)_3\beta_3$ complex against ATP-Mg-induced dissociation

Since it has been reported that the $\alpha_3\beta_3$ complex dissociates into $\alpha_1\beta_1$ heterodimers in the presence of AT(D)P-Mg [8,32,33], the stability of the $\alpha(395/396)_3\beta_3$ complex in the presence of ATP-Mg was examined by native-PAGE and gel-permeation HPLC. As shown in Fig. 6A, a significant population of $\alpha(395/396)_3\beta_3$ complex was electrophoresed without dissociation in the presence of 1 mM ATP-Mg, whereas all of the intact $\alpha_3\beta_3$ complex dissociated into α- and β-subunits (and trace amounts of $\alpha_1\beta_1$ heterodimers) under the same conditions. The protein band of the $\alpha(395/396)_3\beta_3$ complex had an ATPase activity (Fig. 6B). Similar results were obtained from gel-permeation HPLC. When the purified $\alpha(395/396)_3\beta_3$ complex was applied to a gel-permeation column equilibrated with 1 mM ATP-Mg, almost all complexes were eluted without dissociation, whereas about half of intact $\alpha_3\beta_3$ complex dissociated into $\alpha_1\beta_1$ heterodimers under the same conditions (Fig. 6C). Essentially similar results were obtained for ADP-Mg, even though 1 mM ADP-Mg caused more dissociation of $\alpha(395/396)_3\beta_3$ complex. Thus, $\alpha(395/396)_3\beta_3$ complex is more resistant against AT(D)P-Mg-induced destabilization of $\alpha_3\beta_3$ structure than the intact $\alpha_3\beta_3$ complex.

3.8. ATPase activity of the complexes containing $\alpha(395/396)$

As shown in Table 1, the steady-state ATPase activities of $\alpha(395/396)_3\beta_3$ and $\alpha(395/396)_3\beta_3\gamma$ complexes at saturating concentrations of ATP (5 mM) are 177% and 183%, respectively, of the corresponding complexes con-

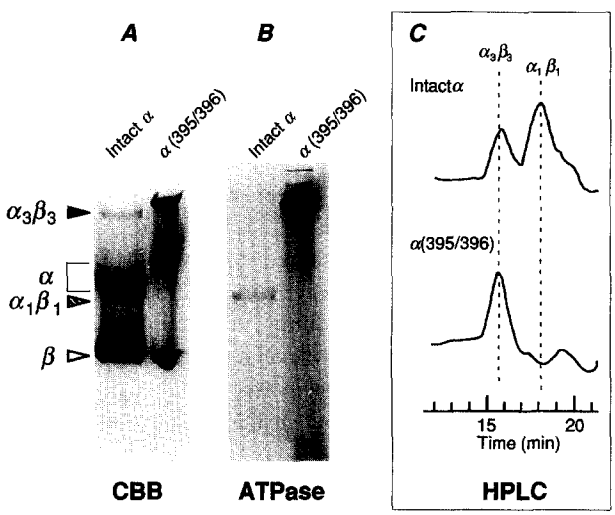

Fig. 6. Native-PAGE analysis of the stability of $\alpha(395/396)_3\beta_3$ complex in the presence of 1 mM ATP-Mg. After a 30 min incubation in 1 mM ATP-Mg, $\alpha_3\beta_3$ complex was analyzed by native-PAGE and HPLC. (A, B) Native-PAGE including 1 mM ATP-Mg in the gel and the buffer of electrophoresis. (A) Stained with Coomassie brilliant blue. (B) ATPase-activity staining on the gel after native-PAGE. Lane 1, intact $\alpha_3\beta_3$ complex. Lane 2, $\alpha(395/396)_3\beta_3$ complex. (C) gel permeation HPLC on a G3000SWXL column equilibrated and eluted with the buffer containing 1 mM ATP-Mg. HPLC elution was monitored by absorbance at 280 nm. Other experimental details are described in Experimental procedures.

Table 1
Steady-state ATPase activities of $\alpha(395/396)_3\beta_3$ and $\alpha(395/396)_3\beta_3\gamma$ complexes

α-Subunit	$\alpha_3\beta_3$ (unit/mg (%))	$\alpha_3\beta_3\gamma$ (unit/mg (%))
Intact α	1.47(100)	6.39(100)
α(395/396)	2.60(177)	11.7(183)

ATPase activities of $\alpha_3\beta_3$ and $\alpha_3\beta_3\gamma$ complexes at 5 mM ATP were measured by enzyme coupling assay and activity at 10 min after initiation of reaction was taken as steady-state activity. The amount of complexes added into 1 ml of the assay mixture was 5 μg. Under the same conditions, the activity of TF_1 was 4.5 unit/mg

taining intact α-subunit. These results provide a solid support for the previous assumption that the stimulated ATPase activity of the $\alpha_3\beta_3$ complex containing proteinase-treated α-subunits was due to a peptide chain nick at the C2-loop region. In addition to the stimulated ATPase activities of $\alpha(395/396)_3\beta_3$ and $\alpha(395/396)_3\beta_3\gamma$ complexes, their kinetics have some altered characteristics which deserve further consideration. When the time-courses of ATP hydrolysis by $\alpha_3\beta_3$ and $\alpha(395/396)_3\beta_3$ complexes are compared, ATP hydrolysis by $\alpha(395/396)_3\beta_3$ complex proceeded linearly with time after initial slow phase, whereas hydrolysis by intact $\alpha_3\beta_3$ complex was slowed down gradually (data not shown). This gradual loss of activity is attributable to AT(D)P-Mg-induced dissociation of the $\alpha_3\beta_3$ complex into ATPase-inactive (or less active) $\alpha_1\beta_1$ complexes. In order to avoid complications arising from dissociation of the $\alpha_3\beta_3$ complexes, kinetic analysis of hydrolytic rate at varying ATP concentrations was carried out for stable $\alpha_3\beta_3\gamma$ complex. Under the assay conditions we used, TF_1 hydrolyzed low concentrations of ATP (< 300 μM) at an accelerated rate in an

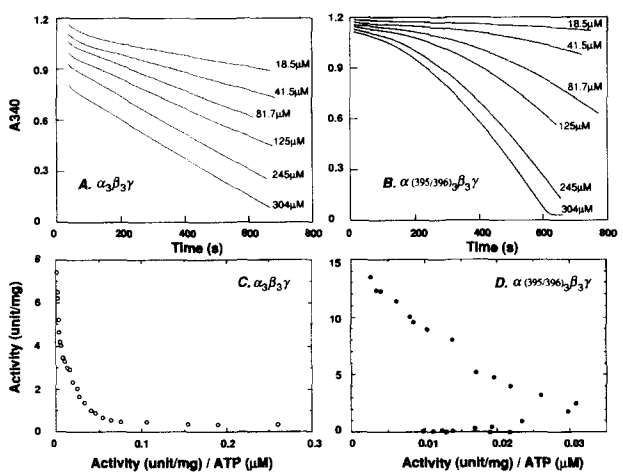

Fig. 7. (A and B) Time-course of ATP hydrolysis by (A) intact $\alpha_3\beta_3\gamma$ complex and (B) $\alpha(395/396)_3\beta_3\gamma$ complex. ATP concentrations are indicated in the figure. The reactions were started by the addition of 4.2 μg of $\alpha_3\beta_3\gamma$ complex or 6.14 μg of $\alpha(395/396)_3\beta_3\gamma$ complex to 1.2 ml of assay mixtures and monitored by the absorbance at 340 nm using enzyme coupling assay. (C and D) Eaddy-Hofstee plots of steady-state ATPase activities of (C) intact $\alpha_3\beta_3\gamma$ complex and (D) $\alpha(395/396)_3\beta_3\gamma$ complex.

initial phase and the rate decreased to reach the steady-state phase. This accelerated initial phase was also observed for the intact $\alpha_3\beta_3\gamma$ complex (Fig. 7A). The duration of accelerated initial phase decreased as the ATP concentration was increased. In contrast, the $\alpha(395/396)_3\beta_3\gamma$ complex exhibited an inhibited initial phase which slowly transformed into a faster steady-state phase. The duration of this inhibited initial phase was more pronounced at low ATP concentrations (Fig. 7B). When the dependency of steady-state ATPase activities on ATP concentration was analyzed with Eaddy-Hofstee plots (Fig. 7C and D), the $\alpha(395/396)_3\beta_3\gamma$ complex showed apparently positive cooperativity in the low ATP concentration range, while the intact $\alpha_3\beta_3\gamma$ complex, similar to native TF_1, showed negative cooperativity. Although the positive cooperativity by the $\alpha(395/396)_3\beta_3\gamma$ complex could be due to underestimation of the steady-state rate caused from a long initial inhibited phase and the real reason for these unusual initial phases is not known, it is obvious that introduction of a peptide chain nick between positions 395 and 396 in the α-subunit has a great effect on the mechanism responsible for cooperative kinetics of F_1-ATPase.

4. Discussion

4.1. α(395/396) maintains native gross structure

It is now clear that, even without a peptide bond between Phe-395 and Ala-396, the amino-terminal and the carboxyl-terminal peptide fragments associate with each other spontaneously to form α(395/396) (Fig. 2) which exhibits apparently normal ability to bind AT(D)P-Mg (Fig. 4). The crystal structure of mitochondrial F_1-ATPase has revealed that the predicted C2-loop is really a loop connecting two α-helices and that the C2-subdomain, which includes a major part of the carboxyl-terminal helical bundle, is in close contact with the ATP-binding domain (Fig. 1) [5]. Nonetheless, it should be added that the gross structure of α(395/396) is less stable than that of the intact α-subunit, since α(395/396) tends to dissociate into two component peptides during native-PAGE (Fig. 3A). The fact that this dissociation is prevented by ATP-Mg (Fig. 3B) indicates that the binding of ATP-Mg induces tighter interaction between these domains.

4.2. The C2-loop is involved in intersubunit conformational communication

Several lines of observations suggest that the C2-loop of the α-subunit is involved in interaction between α- and β-subunits in F_1-ATPase. The $\alpha(395/396)_3\beta_3$ complex is much more resistant than the intact $\alpha_3\beta_3$ complex to AT(D)P-Mg-induced dissociation into $\alpha_1\beta_1$ heterodimers (Fig. 6). This dissociation is likely to be a consequence of the conformational constraint which is induced by ATP

hydrolysis at the catalytic site on the β-subunit. This constraint is transmitted to the α-β interface regions and then causes a certain degree of dissociation of the $\alpha_3\beta_3$ complex. A peptide chain nick at the C2-loop region may contribute to release this conformational constraint without subunit dissociation. In addition to this "physical" effect, introduction of a peptide chain nick at the C2-loop has a significant effect on the "functional" aspect of the enzyme. The ATPase activity of the $\alpha(395/396)_3\beta_3\gamma$ complex is stimulated about 2-fold and obeys a very different type of kinetics from that of the intact $\alpha_3\beta_3\gamma$ complex (Table 1, Fig. 7). The stimulation was also observed for the $\alpha(395/396)_3\beta_3$ complex (Table 1). These results are explained reasonably from the above notion that the C2-loop is involved in α-β-intersubunit conformational communication. The interaction with the γ-subunit can be also mediated by the C2-loop in the $\alpha_3\beta_3\gamma$ complex, since the C2-loop is located at a position close to the central α-helix of the γ-subunit in MF_1 [5]. An intact covalent structure seems necessary for the C2-loop to play a role in these communications.

Acknowledgements

The authors are grateful to Dr. E. Muneyuki for his discussion during this work and his critical reading of the manuscript. This work was supported by a grant-in-aid for scientific research in the priority area of No.04266103 to M.Y. from the Ministry of Education, Science and Culture of Japan.

References

[1] Futai, M., Noumi, T. and Maeda, M. (1989) Annu. Rev. Biochem. 58, 111–136.
[2] Senior, A.E. (1990) Annu. Rev. Biophys. Chem. 19, 7–41.
[3] Penefsky, H.S. and Cross, R.L. (1991) Adv. Enzymol. Relat. Areas Mol. Biol. 64, 173–214.
[4] Boyer, P.D. (1993) Biochim. Biophys. Acta 1140, 215–250.
[5] Abrahams, J.P., Leslie, A.G.W., Lutter, R. and Walker, J.E. (1994) Nature 370, 621–628.
[6] Tozawa, K., Miyauchi, M. and Yoshida, M. (1993) J. Biol. Chem. 268, 19044–19054.
[7] Miwa, K. and Yoshida, M. (1989) Proc. Natl. Acad. Sci. USA 86, 6484–6487.
[8] Kagawa, Y., Ohta, S. and Otawara-Hamamoto, Y. (1989) FEBS Lett. 249, 67–69.
[9] Andralojc, P.J. and Harris, D.A. (1993) Biochim. Biophys. Acta 1143, 51–61.
[10] Odaka, M., Kaibara, C., Amano, T., Matsui, T., Muneyuki, E., Ogasawara, K., Yutani, K. and Yoshida, M. (1994) J. Biochem. 115, 789–796.
[11] Rao, R., Pagan, J. and Senior, A.E. (1988) J. Biol. Chem. 263, 15957–15963.
[12] Walker, J.E., Saraste, M., Runswick, M.J. and Gay, N.J. (1982) EMBO J. 1, 945–951.
[13] Yohda, M., Ohta, S., Hisabori, T. and Kagawa, Y. (1988) Biochim. Biophys. Acta 933, 156–164.
[14] Jault, J.-M., Di Pietro, A., Falson, P. and Gautheron, D.C. (1991) J. Biol. Chem. 266, 8073–8078.
[15] Soga, S., Noumi, T., Takeyama, M., Maeda, M. and Futai, M. (1989) Arch. Biochem. Biophys. 268, 643–648.
[16] Lee, R.S.-F., Wilke-Mounts, S. and Senior, A.E. (1992) Arch. Biochem. Biophys. 297, 334–339.
[17] Maggio, M.B., Pagan, J., Parsonage, D., Hatch, L. and Senior, A.E. (1987) J. Biol. Chem. 262, 8981–8984.
[18] Turina, P., Aggeler, R., Lee, R.S.F., Senior, A.E. and Capaldi, R.A. (1993) J. Biol. Chem. 268, 6978–6984.
[19] Noumi, T., Futai, M. and Kanazawa, H. (1984) J. Biol. Chem. 259, 10076–10079.
[20] Weber, J., Lee, R.S.-F., Wilke-Mounts, S., Grell, E. and Senior, A.E. (1993) J. Biol. Chem. 268, 6241–6247.
[21] Dunn, S.D., Heppel, L.A. and Fullmer, C.S. (1980) J. Biol. Chem. 255, 6891–6896.
[22] Maggio, M.B., Personage, D. and Senior, A.E. (1988) J. Biol. Chem. 263, 4619–4623.
[23] Date, T., Tanihira, K. and Numura, N. (1990) Gene 90, 141–144.
[24] Kunkel, T.A., D. Robert, J. and Zakour, R.A. (1987) Methods Enzymol. 154, 367–382.
[25] Ohtsubo, M., Yoshida, M., Ohta, S., Kagawa, Y., Yohda, M. and Date, T. (1987) Biochem. Biophys. Res. Commun. 146, 705–710.
[26] Yoshida, M., Sone, N., Hirata, H. and Kagawa, Y. (1977) J. Biol. Chem. 252, 3480–3485.
[27] Laemmli, U.K. (1970) Nature 227, 680–685.
[28] Ohta, S., Harada, M., Ito, Y., Kobayashi, Y., Sone, N. and Kagawa, Y. (1990) Biochem. Biophys. Res. Commun. 171, 1258–1263.
[29] Bradford, M.M. (1976) Anal. Biochem. 72, 248–254.
[30] Tozawa, K., Odaka, M., Date, T. and Yoshida, M. (1992) J. Biol. Chem. 267, 16484–16490.
[31] Hisabori, T., Yoshida, M. and Sakurai, H. (1986) J. Biochem. 100, 663–670.
[32] Harada, M., Ito, Y., Sato, M., Aono, O., Ohta, S. and Kagawa, Y. (1991) J. Biol. Chem. 266, 11455–11460.
[33] Kagawa, Y., Ohta, S. (1992) Ann. N.Y. Acad. Sci. 671, 366–376.